Low Complexity MMSE Receivers for Multirate DS-CDMA Systems[1]

Ashutosh Sabharwal
Department of Electrical and Computer Engineering
Rice University
Houston TX 77005

Urbashi Mitra and Randolph Moses
Department of Electrical Engineering
The Ohio State University
Columbus OH 43210

Abstract — **Low-complexity minimum-mean squared error (MMSE) receivers are designed and analyzed for multiple data rate direct-sequence code division multiple access (DS-CDMA) systems. In a previous paper, it was shown that the optimal MMSE receiver for multirate DS-CDMA systems may be periodically time-varying. When the period of the optimal receiver is large, the optimal MMSE receiver may have prohibitive complexity. In this paper, suboptimal receivers are proposed to achieve a lower complexity implementation. The proposed receivers are designed as a function of the cyclic statistics of the signals. Simulations show that significant performance gains are realized by the proposed periodically time-varying MMSE receivers over their time-invariant counterparts. It is also observed that near optimal perforamance can be achieved by the reduced complexity receivers.**

I. Introduction

Direct sequence code division multiple access (DS-CDMA) is a promising technique for providing multi-user access in wireless systems. Past efforts to create robust and efficient receivers for DS-CDMA communication had been driven by the current cellular telephony network and thus focused on constant bit rate traffic such as voice [1–3]. With the exploding growth of cellular communication systems, there has been a considerable interest in the provision of wireless transport for a variety of data sources, including images (facsimiles), video, data, and voice. To serve sources with inherently different information rates in a wireless system, it is desirable to develop multiple data rate systems [4, 5].

Among the receivers proposed for multi-rate DS-CDMA systems are the conventional receiver [6], decorrelator-based receivers [7–9], minimum-mean-squared error receivers [10], the optimum receiver [11], and receivers based on successive interference cancellation [12]. Much of the prior work on multi-rate receiver design assumed a constant chipping rate, with multi-rate access being achieved by varying the spreading gain or by multiplexing the high rate traffic [5, 13].

In [10, 14], the optimal MMSE receiver was designed for multiple data rate CDMA systems, which was shown to be periodic in most cases of interest. The complexity of linear MMSE receivers in future systems with variable symbol periods will be governed by two major factors: periodicity of the receiver[2], and length of the receiver. The length of the receivers is in turn dependent on the sampling rate, or equivalently, on the front-end filter bandwidth. The effect of the front-end filter bandwidth in multiple bandwidth systems was studied in [14]. In this paper, we derive low complexity suboptimal MMSE receivers for multiple rate DS-CDMA systems. The suboptimal MMSE receivers, of which the time-invariant MMSE receiver is a special case, can offer near-optimal performance in some cases.

The inherent cyclostationarity of the multirate signal is exploited to construct the MMSE receivers. Cyclostationarity of the received DS-CDMA signal was inherently exploited in [10] to obtain optimal MMSE receivers for a dual rate system; the role of cyclostationarity was made explicit in [14] to derive the optimal MMSE receiver for multiclass systems. While a time domain derivation of the optimal MMSE receiver was provided in [10], we have relied on a frequency domain representation in [14] and in this paper. Furthermore, we derive MMSE receivers without any causality constraints; this extends the work in [15, 16] to data demodulation for multirate signals. The primary motivation for not imposing causality constraints is to learn the structure of optimal MMSE receivers, thus this work is a necessary precursor to considering practical, adaptive (possibly blind), causal implementations. The proposed framework is applicable to DS-CDMA systems with multiple spreading gains, multiple chipping rates and multicarrier transmission, in the presence of multipath. The suboptimal MMSE receivers, of which the time-invariant MMSE receiver is a special case, can offer near-optimal performance in some cases.

The rest of paper is organized as follows. In Section II, the signal model is described and the cyclostationarity of the received signal is briefly reviewed. In Section III, we derive the proposed suboptimal MMSE receivers and compute the achievable mean-squared error. For a given receiver complexity, there is more than one choice of suboptimal receiver. We also consider the choice of suboptimal receivers in Section III. Brief numerical results for a three class system are given in Section IV. Finally, some conclusions are provided in Section V.

II. Signal model

For simplicity of presentation, we assume that all users use the same carrier frequency; multicarrier systems are considered in [17]. The methods considered in the current work are applicable to multiple carrier systems without any modification.

[1] This work was supported in part by an Ameritech Dissertation Fellowship and the National Science Foundation under CAREER Grant NCR 96-24375.

[2] Multirate traffic in the next generation systems will range from tens of kilobits per second to roughly 2 Mb/s [4].

The received baseband signal is

$$y(t) = \sum_{k=1}^{C}\sum_{i=1}^{P_k} A_{ik}x_{ik}(t) + \eta(t) \quad (1)$$

where $x_{ik}(t) = \sum_{l=-\infty}^{\infty} b_{ik}(l)s_{ik}(t - lT_k - \tau_{ik})$.The number of service classes is denoted by C; each class corresponds to a different symbol period. There are P_k users in class k. Each user in a particular class transmits at the same symbol rate, $\frac{1}{T_k}$, with spreading gain L_{ik}. Users are indexed by two variables: k indicates the class and i indicates the user number within class k. The received signal for user ik is denoted by $x_{ik}(t)$. The corresponding received amplitude is A_{ik}. Each user ik is received after a propagation delay of τ_{ik}. The additive noise process, $\eta(t)$, is assumed to be white and stationary with zero mean and power $\frac{N_o}{2}$. The information stream for user ik is denoted by $b_{ik}(l)$ and $\mathbb{E}\left\{|b_{ik}(l)|^2\right\} = 1$. For simplicity of presentation, BPSK modulation is assumed. The information bits are assumed to be independent from user to user and in time. The effective spreading waveform is denoted by $s_{ik}(t)$ and is the convolution of the multipath, $m_{ik}(t)$, and the actual spreading waveform; the actual spreading waveform is formed by modulating a pseudo-random noise sequence, $a_{ik}(n)$, with the pulse shape $\phi_{ik}(t)$:

$$s_{ik}(t) = \underbrace{m_{ik}(t)}_{\text{multipath}} \circledast \underbrace{\sum_{n=1}^{L_{ik}} a_{ik}(n)\phi_{ik}\left(t - nT_{c_{ik}}\right)}_{\text{actual spreading waveform}}$$

such that $\| \sum_{n=1}^{L_{ik}} a_{ik}(n)\phi_{ik}\left(t - nT_{c_{ik}}\right) \| = 1$. The convolution operator is denoted by $\circledast$. The chip duration of class k is T_{c_k} where $T_{c_{ik}} = \frac{T_k}{L_{ik}}$. Arbitrary pulse shapes, $\phi_{ik}(t)$, are considered herein, but in practice, bandlimited pulses are used[3].

The autocorrelation of the received multirate signal, $y(t)$ in (1) is

$$R_y(t,u) = \sum_{k=1}^{C}\sum_{i=1}^{P_k} A_{ik}^2 R_{ik}(t,u) + R_\eta(t-u), \quad (2)$$

where $R_{ik}(t,u)$ is the covariance of $x_{ik}(t)$, and is periodic with period T_k. The covariance function of $\eta(t)$ is denoted by $R_\eta(t-u)$. Under the assumption of equally probable bits, the covariance of $x_{ik}(t)$ can be computed as follows

$$\begin{aligned} R_{ik}(t,u) =& \mathbb{E}\left\{x_{ik}^2(t)\right\} \\ =& A_{ik}^2 \sum_{n=-\infty}^{\infty} R_b(n) \sum_{l=-\infty}^{\infty} s_{ik}(t-lT)s_{ik}(u-lT-nT), \end{aligned}$$

where $R_b(n)$ is the correlation of the stationary data sequence. For i.i.d. data, $R_b(n) = \delta_n$, where the Kronecker delta function $\delta_n = 1$ if $n = 0$ and zero otherwise. Note that $R_{ik}(t + T_k, u + T_k) = R_{ik}(t,u)$. The periodicity of $R_y(t,u)$ depends on the ratio of individual symbol periods, T_k. For the rest of the paper, we assume that the least common multiple, $T = \text{LCM}(T_1, T_2, \ldots, T_k)$, exists and hence is finite. If T is finite, the period of $R_y(t,u)$ is T, *i.e.*, $R_y(t + kT, u + kT) = R_y(t,u)\ \forall k$. Finally, we define the constants, $v_k = \frac{T}{T_k}$; clearly, $v_k \in \mathbb{Z}^+$.

[3]Rectangular pulse shapes and thus very wide bandwidth front end filters are assumed in [10].

III. Proposed MMSE Receivers

The desired linear receiver structure is shown in Figure 1, where $h(t)$ is the front-end filter. The front end filter, $h(t)$, is assumed to be a linear and time-invariant, and its bandwidth is chosen based on the sampling period. The MMSE receiver, $u(t,l)$, is constrained to be linear, but no constraint on time-invariance or causality is imposed. Further, we consider symbol-by-symbol demodulation, *i.e.*, symbol decisions are made at the end of each symbol.

A Suboptimal Receivers

In [14], it was shown that the optimal MMSE receiver may be periodically time-varying, by decomposing each user into several virtual users to convert the problem into a single rate multiuser problem. This implies that the optimal time-varying receiver admits a Fourier series representation,

$$\begin{aligned} U_l^\circ(f) &= U_{l+v_1}^\circ(f) \\ &= \sum_{\alpha=0}^{v_1-1} \psi_\alpha^\circ(f) e^{-j2\pi\frac{\alpha}{v_1}l}, \end{aligned} \quad (3)$$

where $U_l(f)$ is the Fourier transform of $u(t,l)$. The reduced complexity receivers are obtained by truncating the series,

$$U_l(f) = \sum_{\alpha\in\Omega} \psi_\alpha(f) e^{-j2\pi\frac{\alpha}{v_1}l}, \quad (4)$$

where $\Omega = \{\alpha_1, \alpha_2, \ldots, \alpha_\lambda\} \subset \{0, 1, \ldots, v_1 - 1\}$. Note that $U_l(f) = U_{l+v_1}(f)$; v_1 may be a multiple of the actual period of $U_l(f)$.

Without loss of generality, we consider user 1 in class 1, *i.e.*, user 11; the symbol period of user 11 is T_1. The soft symbol estimates are obtained by sampling the output of a linear receiver (4) at $t = lT_1$,

$$\hat{b}_{11}(i) = \sum_{\alpha\in\Omega} \int Y(f)\psi_\alpha(f) e^{-j2\pi\frac{\alpha}{v_1}i} e^{-j2\pi f i T_1} df, \quad (5)$$

where $Y(f)$ is the Fourier transform of $y(t)$. Actual bit estimates are obtained by hard limiting the soft estimates, $\hat{b}_{11}(l)$, to the closest symbol. The objective is to minimize the mean-squared error between the true data symbols and their soft estimates,

$$\{u_\alpha^\circ(t)\}_{\alpha\in\Omega} \ = \ \arg \min_{\{u_\alpha(t)\}_{\alpha\in\Omega}} \mathbb{E}_l\, \mathbb{E}_b \|b_{11}(l) - \hat{b}_{11}(l)\|^2, \quad (6)$$

where $\mathbb{E}_l$ is the time average and $\mathbb{E}_b$ is the ensemble average. The reason for introducing the time average, $\mathbb{E}_l$, is to account for the time-variation of the linear receiver output. In [17], it is shown that (6) is equal to the following

$$\{\psi_\alpha^\circ(f)\} = \arg \min_{\{\psi_\alpha(f)\}} \sum_{i=0}^{v_1-1} \mathbb{E}_b \|b_{11}(i) - \hat{b}_{11}(i)\|^2. \quad (7)$$

The key steps of the derivation are reproduced below; more details can be found in [17]. Denote the Fourier transform of $h(t)$ and $s_{ik}(t - \tau_{ik})$ by $H(f)$ and $S_{ik}(f)$, respectively. Let $V_d(f) = \mathbb{E}\{b_{11}(d)Y^*(f)\}$. Define the vector of Fourier transformed signature waveforms of all the virtual users [14] corresponding to user ik,

$$q_{ik}(f) = H(f)S_{ik}(f) \begin{bmatrix} 1 \\ e^{-j2\pi f T_k} \\ e^{-j2\pi f 2T_k} \\ \cdots \\ e^{-j2\pi f(v_k-1)T_k} \end{bmatrix}_{v_k\times 1}.$$

Further define the (super)vector of all P virtual users,

$$\mathcal{Q}_k(f) = \begin{bmatrix} q_{1k}^T(f) \\ \cdots \\ q_{P_k k}^T(f) \end{bmatrix}_{v_k P_k \times 1},$$

$$\mathcal{Q}(f) = \begin{bmatrix} \mathcal{Q}_1^T(f) \\ \cdots \\ \mathcal{Q}_C^T(f) \end{bmatrix}_{P \times 1}.$$

Also define

$$\begin{aligned}
\Gamma_y(f, f') &= \mathbb{E}\{Y(f) Y^*(f')\} \\
&= \frac{1}{T} \sum_{n=-\infty}^{\infty} \gamma_y^{(n)}(f) \delta\left(f - f' - \frac{n}{T}\right), \\
\gamma_y^{(n)}(f) &= \mathcal{Q}^T(f) \mathbf{A} \mathcal{Q}^*\left(f - \frac{n}{T}\right), \\
V_d(f) &= \mathcal{Q}^T(f) \mathcal{B}_d, \quad d = 0, \ldots, v_1 - 1.
\end{aligned}$$

The $P \times 1$ vector $\mathcal{B}_d$ is a vector of zeros except for the $(d+1)^{st}$ location which is equal to A_{11} and

$$\begin{aligned}
\mathbf{a}_{ik} &= A_{ik}^2 \mathbf{I}_{v_k}, \\
\mathbf{A}_k &= \operatorname{diag}\left(\mathbf{a}_{1k}, \ldots, \mathbf{a}_{P_k k}\right)_{P_k v_k \times P_k v_k}, \\
\mathbf{A} &= \operatorname{diag}\left(\mathbf{A}_1, \ldots, \mathbf{A}_C\right)_{P \times P},
\end{aligned}$$

where $\mathbf{I}_{v_k}$ is the $v_k \times v_k$ identity matrix. The optimal $\psi^\circ(f)$ should satisfy the following first order optimality condition [18] for $\alpha \in \Omega$,

$$\sum_{i=0}^{v_1-1} e^{\jmath 2\pi \frac{\alpha}{v_1} i} \left[\int \Gamma_y^*(f, f') \left(\sum_{\alpha'} \psi_{\alpha'}^\circ(f') e^{-\jmath 2\pi \frac{\alpha'}{v_1} i} \right) e^{-\jmath 2\pi (f - f') i T_1} df' + \frac{N_o}{2} |H(f)|^2 \sum_{\alpha'} \psi_{\alpha'}^\circ(f) e^{-\jmath 2\pi \frac{\alpha'}{v_1} i} \right] = \sum_{i=0}^{v_1-1} e^{\jmath 2\pi \frac{\alpha}{v_1} i} V_0(f), \tag{8}$$

which simplifies to

$$\sum_{\alpha'} \left[\int \Gamma_y^*(f, f') \psi_{\alpha'}^\circ(f) \sum_{i=0}^{v_1-1} e^{\jmath 2\pi \frac{(\alpha - \alpha')}{v_1} i} e^{-\jmath 2\pi (f - f') i T_1} df + \delta_{\alpha - \alpha'} \frac{N_o}{2} |H(f)|^2 \psi_{\alpha'}^\circ \right] = \delta_\alpha V_0(f), \ \ \alpha \in \Omega. \tag{9}$$

By using the cyclostationarity of $y(t)$, we obtain for $\alpha \in \Omega$

$$\sum_{\alpha'} \left[\frac{1}{T} \sum_{k=-\infty}^{\infty} \left[\gamma_y^{(kv_1 + \alpha' - \alpha)}\right]^* \psi_{\alpha'}^\circ \left(f - \frac{kv_1 + \alpha' - \alpha}{T}\right) + \delta_{\alpha - \alpha'} \frac{N_o}{2} |H(f)|^2 \psi_{\alpha'}^\circ \right] = \delta_\alpha V_0(f). \tag{10}$$

It is easy to verify that $\psi_\alpha^\circ(f)$ can be written as [16, 17] $\psi_\alpha^\circ(f) = \mathcal{Q}^H(f) \frac{\xi_\alpha(f)}{|H(f)|^2}, \alpha = \Omega$, where $\xi_\alpha(f)$ is a $P \times 1$ vector with periodic entries, each with period $v_1/T = 1/T_1$. We define

$$\mathbf{S}_r(f) = \frac{\mathbf{A}}{T} \sum_{k=-\infty}^{\infty} \frac{\mathcal{Q}\left(f - \frac{kv_1 + r}{T}\right) \mathcal{Q}^H\left(f - \frac{kv_1 + r}{T}\right)}{\left|H\left(f - \frac{kv_1 + r}{T}\right)\right|^2}$$

to concisely write (10) as

$$\sum_{\substack{\alpha' \in \Omega \\ \alpha' \neq \alpha}} \mathbf{S}_{\alpha' - \alpha}\left(f - \frac{\alpha}{T}\right) \xi_{\alpha'}\left(f - \frac{\alpha'}{T}\right) + \underbrace{\left(S_0\left(f - \frac{\alpha}{T}\right) + \frac{N_o}{2}\mathbf{I}\right)}_{\overline{\mathbf{S}}_0\left(f - \frac{\alpha}{T}\right)} \xi_\alpha\left(f - \frac{\alpha}{T}\right) = \delta_\alpha \mathcal{B}_0. \tag{11}$$

A sufficient condition required to conclude (11) from (10) is that the signature waveforms of all the virtual users are linearly independent [16]. Also it suffices to consider $f \in [0, 1/T_1]$ since both $\mathbf{S}_r(f)$ and $\xi_\alpha(f)$ are periodic with period $1/T_1$. Furthermore it is easy to verify that $\mathbf{S}_{v_1 - r}(f) = \mathbf{S}_{-r}(f)$. Thus, the $\lambda P \times 1$ interference suppression vector $\left[\xi_{\alpha_1}^T\left(f - \frac{\alpha_1}{T}\right) \cdots \xi_{\alpha_\lambda}^T\left(f - \frac{\alpha_\lambda}{T}\right)\right]^T$ can be obtained by solving

$$\Theta_{\lambda P \times \lambda P} \boldsymbol{\xi}_{\lambda P \times 1} = \boldsymbol{\delta}_{\lambda P \times 1} \tag{12}$$

where

$$\Theta = \begin{bmatrix}
\overline{\mathbf{S}}_0\left(f - \frac{\alpha_1}{T}\right) & \mathbf{S}_{21}\left(f - \frac{\alpha_1}{T}\right) & \cdots & \mathbf{S}_{\lambda 1}\left(f - \frac{\alpha_1}{T}\right) \\
\mathbf{S}_{12}\left(f - \frac{\alpha_2}{T}\right) & \overline{\mathbf{S}}_0\left(f - \frac{\alpha_2}{T}\right) & \cdots & \mathbf{S}_{\lambda 2}\left(f - \frac{\alpha_2}{T}\right) \\
\vdots & & & \vdots \\
\mathbf{S}_{1\lambda}\left(f - \frac{\alpha_\lambda}{T}\right) & \mathbf{S}_{2\lambda}\left(f - \frac{\alpha_\lambda}{T}\right) & \cdots & \overline{\mathbf{S}}_0\left(f - \frac{\alpha_\lambda}{T}\right)
\end{bmatrix}$$

$$\boldsymbol{\xi} = \begin{bmatrix} \xi_{\alpha_1}\left(f - \frac{\alpha_1}{T}\right) \\ \xi_{\alpha_2}\left(f - \frac{\alpha_2}{T}\right) \\ \vdots \\ \xi_{\alpha_\lambda}\left(f - \frac{\alpha_\lambda}{T}\right) \end{bmatrix}, \quad \boldsymbol{\delta} = \begin{bmatrix} \delta_{\alpha_1} \mathcal{B}_0 \\ \delta_{\alpha_2} \mathcal{B}_0 \\ \vdots \\ \delta_{\alpha_\lambda} \mathcal{B}_0 \end{bmatrix}.$$

with $\mathbf{S}_{km}(f) = \mathbf{S}_{\alpha_k - \alpha_m}(f)$. If $\alpha = 0 \notin \Omega$, then MMSE optimization (7) has a trivial solution; all filters equal to zero. This implies that to have a useful suboptimal solution, the zeroth cycle frequency, $\alpha = 0$, should always be included in the optimization for suboptimal receivers. Further, the smallest set Ω which yields a non-trivial solution is $\Omega = \{0\}$, the time-invariant solution. Equivalently, the time-invariant solution can be derived from Wiener-Hopf equations by only using the zeroth cyclic spectrum.

Consider the case of $v_1 = 2$ for $\Omega_1 = \{0\}$ and $\Omega_2 = \{1\}$. Corresponding to the sets Ω_1 and Ω_2, the matrix equation (12) yields

$$\begin{aligned}
\xi_0(f) &= \overline{\mathbf{S}}_0^{-1}(f) \mathcal{B}_0, \quad \text{for } \Omega_1 = \{0\} \\
\xi_1(f) &= \overline{\mathbf{S}}_0^{-1}(f) 0 = 0, \quad \text{for } \Omega_2 = \{1\}
\end{aligned}$$

Clearly, the zeroth cycle frequency must be included in Ω. The above suboptimal receivers can be compared with the optimal MMSE receiver [17], which is given by the following set of equations. The matrix equation (12) for $\lambda = 2$ is

$$\begin{bmatrix} \overline{\mathbf{S}}_o(f) & \mathbf{S}_1(f) \\ \mathbf{S}_1\left(f - \frac{1}{T}\right) & \overline{\mathbf{S}}_0\left(f - \frac{1}{T}\right) \end{bmatrix} \begin{bmatrix} \xi_0(f) \\ \xi_1\left(f - \frac{1}{T}\right) \end{bmatrix} = \begin{bmatrix} \mathcal{B}_0 \\ 0 \end{bmatrix},$$

which implies

$$\begin{aligned}
\xi_0(f) &= \left(\overline{\mathbf{S}}_0(f) - \mathbf{S}_1(f) \overline{\mathbf{S}}_0\left(f - \frac{1}{T}\right)^{-1} \mathbf{S}_1\left(f - \frac{1}{T}\right) \right)^{-1} \mathcal{B}_0 \\
\xi_1(f) &= \overline{\mathbf{S}}_0^{-1}(f) \mathbf{S}_1(f) \xi_0\left(f - \frac{1}{T}\right).
\end{aligned}$$

Note that $\xi_1(f)$ is a function of $\xi_0(f)$.

B Performance analysis

The MSE achieved by the proposed suboptimal receivers, $\epsilon_{\min}(\Omega)$, is given by

$$\begin{aligned}\epsilon_{\min}(\Omega) &= 1-\sum_{\alpha\in\Omega} v_1\delta_\alpha \int V_0^*(f)\psi_\alpha^\circ(f)df. \\ &= 1-v_1T\int_0^{v_1/T} \mathcal{B}_0^T\mathbf{A}^{-1}\mathbf{S}_0(f)\xi_0(f)df. \quad (13)\end{aligned}$$

The mean-squared error expression (13) can be rewritten in terms of $\xi_\alpha(f)$ by using (11),

$$\begin{aligned}\epsilon_{\min}(\Omega) =& 1-v_1T\int_0^{v_1/T} \mathcal{B}_0^T\mathbf{A}^{-1}\mathbf{S}_0(f)\overline{\mathbf{S}}_0^{-1}(f) \\ &\left[\mathcal{B}_0-\sum_{\substack{\alpha'\in\Omega\\ \alpha'\neq 0}}\mathbf{S}_{\alpha'}(f)\,\xi_{\alpha'}\left(f-\frac{\alpha'}{T}\right)\right]df. \quad (14)\end{aligned}$$

Note that the first two terms denote the MSE achieved by the optimal time-invariant MMSE receiver, and the last term is the extra reduction in the MSE achieved by introducing additional cycle frequencies.

C Choice of cycle frequencies

From the discussion in the Section IV(B), it is clear that the zeroth cycle frequency should always be a member of Ω. Given a bound on the number of cycle frequencies, λ_o, which can be used, an obvious approach to find the best subset of $\{0,1,\ldots,v_1-1\}$ is an exhaustive search over all possible $\binom{v_1}{\lambda_o-1}$ subsets of cycle frequencies[4].

Two heuristic methods of choosing the best subset, Ω, of a given cardinality, λ_o, are as follows. The first method requires calculating the Fourier coefficients for the optimal time-varying receiver and retaining the cycle frequencies corresponding to the strongest λ_o coefficients. This requires computation of the optimal receiver, computation of which may have prohibitive complexity. The second heuristic can be obtained by inspecting (14). Observe that the mean-squared error contribution of each Fourier coefficient, $\epsilon_{\alpha'}(\Omega)$ is

$$\begin{aligned}\epsilon_{\alpha'}(\Omega) & \\ \leq\ & v_1T\int_0^{v_1/T}\|\mathcal{B}_0\|_\varrho \left\|\left|\mathbf{A}^{-1}\mathbf{S}_0(f)\overline{\mathbf{S}}_0^{-1}(f)\mathbf{S}_{\alpha'}(f)\right\|\right|_\varrho \\ & \left\|\xi_{\alpha'}\left(f-\frac{\alpha'}{T}\right)\right\|_\varsigma df \\ \leq\ & \kappa\int_0^{v_1/T}\left\|\left|\mathbf{A}^{-1}\mathbf{S}_0(f)\overline{\mathbf{S}}_0^{-1}(f)\mathbf{S}_{\alpha'}(f)\right\|\right|_\varrho df \\ =\ & \kappa\int_0^{v_1/T}\||\mathbf{J}_{\alpha'}(f)\||_\varrho\, df, \quad (15)\end{aligned}$$

where we have used the Schwarz and Holder inequality [20] such that $\varrho\geq 1$ and $\frac{1}{\varrho}+\frac{1}{\varsigma}=1$. Here $\|\cdot\|_\varrho$ is ϱ-vector norm and $\||\cdot\||_\varrho$ is the corresponding vector induced matrix norm. Also, the constant $\kappa = v_1T\|\mathcal{B}_0\|_\varrho\sup_{f,\alpha'\in\Omega\backslash 0}\|\xi_{\alpha'}(f)\|_\varsigma$ and $\mathbf{J}_{\alpha'}(f) = \mathbf{A}^{-1}\mathbf{S}_0(f)\overline{\mathbf{S}}_0^{-1}(f)\mathbf{S}_{\alpha'}(f) = \mathbf{A}^{-1}\mathbf{S}_0(f)\overline{\mathbf{S}}_0^{-1}(f)\mathbf{S}_0\left(f-\frac{\alpha'}{T}\right)$, using the definition of $\mathbf{S}_r(f)$. The above bound on the mean-squared error contribution of each Fourier coefficient requires computation of only $\mathbf{S}_0(f)$ and choosing cycle frequencies based on the magnitude of the norm $\int_0^{v_1/T}\||\mathbf{J}_{\alpha'}(f)\||_\varrho\, df$; hence, this technique has a lower computational complexity than truncating the Fourier series of the optimal receiver. In all our simulations, all three methods of choosing the best subset of cycle frequencies of a given size, *i.e.*, exhaustive search, magnitude of the Fourier filters and using the induced norm in (15), led to the same solution.

[4]A systematic non-exhaustive technique to choose an appropriate subset of cycle frequencies has proved to be elusive so far [19, and references therein].

IV. Numerical Results

In this section, we provide representative simulation results to verify the performance of the proposed receivers. A three class multirate multiuser scenario in the presence of multipath is considered to compare the performance of the suboptimal MMSE receivers with the optimal MMSE receiver.

The symbol periods of the three user classes are chosen to be $T_1=1$, $T_2=2$, $T_3=4$. The spreading gain of users in Classes 1, 2 and 3 are $L_{k_1 1}=16$, $L_{k_2 2}=32$ and $L_{k_3 3}=32$, $k_i=1,\ldots,P_i$, $i=1,2,3$. With these parameters, users in Classes 1 and 2 have the same bandwidth, but different information rates. The total number of users in the system is 11, with $P_1=3$, $P_2=4$ and $P_3=4$. Further, all users in all classes have the same amplitude, $A_{ik}=1$. The delay for each user is chosen randomly and varied from zero to two chips. Each user employs a raised cosine pulse with rolloff of 0.5, to allow a discrete time implementation. The sampling period is chosen to be $\frac{1}{4}$. Thus, we consider a mixed variable chipping rate, variable spreading length, single carrier system.

Each user encounters a different multipath channel, which is randomly generated as follows. The delay spread of the channel is fixed, which implies that the number of taps in the discrete time representation of the channels is the same for all users because the sampling rate is the same for all users. The length of the discrete time representation of each channel is chosen to be 8, which is equal to 2 chips for Class 1, 2 chips for Class 2 and 1 chip for Class 3. The actual realization of the channel for each user is obtained by adding a random vector (independent, identically distributed with a uniform distribution on $[0,0.1]$) to the following 8-tap channel, $[1\ \ .3\ \ .2\ \ -.15\ \ -.1\ \ -.1\ \ -.01\ \ .01]$.

The probability of error performance as a function of SNR for users 11, 12, 13 is shown in Figures 2-4. The curves are labeled with cycle frequencies used, *e.g.*, 013 means that the zeroth, first and third cycle frequencies were used. The period of the optimal MMSE receiver for users in Classes 1, 2 and 3 are 4, 2 and 1, respectively; thus, the number of nontrivial suboptimal receivers obtained by using a reduced set of cycle frequencies is 7, 1 and 0, for users in Classes 1, 2 and 3, respectively.

Consider the performance of user 11 in Figure 2. From Figure 2, it is clear that cycle frequency 2 is the most important among $\{1,2,3\}$. Because of the conjugate symmetry, cycle frequencies 1 and 3 can be exchanged without affecting the results. The following can be concluded from Figure 2.

1. Each additional cycle frequency leads to improved performance. The performance increases monotonically for the sets 0, 01, 012 and 0123.

2. A smaller set of cycle frequencies may outperform a larger set of different cycle frequencies. The performance for the set 02 is better than for 013.

3. The time-invariant receiver can be considerably worse in performance than the optimal receiver, and most of the performance loss may be recoverable by a moderate increase in complexity (*i.e.*, by including a modest number of cycle frequencies). The set 02 performs considerably better than the time-invariant receiver, and only about 2 dB away from the optimal MMSE receiver.

4. The normalized 2-norm of the filter coefficients may be good predictors of suboptimal receiver performance, for example, $\|\psi_l(f)\|_2$, at SNR=12dB, are [1, 0.1249, 0.4150, 0.1249]. The second cycle frequency coefficient is three times in magnitude as that of the first and third cycle frequency coefficients. The combined magnitude of $\psi_1(f)$ and $\psi_3(f)$ is less than that of $\psi_2(f)$, thereby suggesting that the cycle frequency set 02 may outperform the set 013, which is supported by the results in Figure 2. The normalized matrix norm in (15) also follows a similar trend; they are [1, 0.2704, 0.6024, 0.2704] for $\varrho = 1$ and $\varsigma = \infty$. The choice of $\varrho = 1$ and $\varsigma = \infty$ is *ad-hoc* and was found to be the most accurate predictor of the performance among different values of ϱ. It is conjectured that the sup-norm ($\varsigma = \infty$) on the filter coefficients makes the inequalities tighter, leading to better estimates of the mean-squared error contributions of different filter coefficients.

V. Conclusions

In this paper, we have derived low-complexity suboptimal linear MMSE receiver for multiple data rate communications, with applications to multirate DS-CDMA and multicarrier systems. The proposed receiver structure applies to signals with arbitrary multiple chipping rates and spreading gains. It was shown that the time-invariant receiver may suffer a significant loss as compared to the optimal MMSE receiver and most of this loss may be recovered by a moderate increase in complexity.

Acknowledgments

The authors will like to thank Abhay Sharma and Anshul Sharma of the Ohio State University for their generous help with computer simulations.

References

[1] S. Verdú, *Multiuser Detection.* Cambridge University Press, 1998.

[2] A. Duel-Hallen, "Decorrelating decision-feedback multiuser detector for synchronous Code-Division Multiple-Access Channels," *IEEE Trans. on Comm.*, vol. 41, pp. 285–290, February 1993.

[3] U. Madhow and M. L. Honig, "MMSE inteference suppression for direct-sequence spread-spectrum CDMA," *IEEE Trans. Comm.*, vol. 42, no. 12, pp. 3178–3188, 1994.

[4] E. Dahlman, B. Gudmundson, M. Nilsson, and J. Sköld, "UMTS/IMT2000 based on wideband CDMA," *IEEE Communications Magazine*, pp. 70–80, September 1998.

[5] F. Adachi, M. Sawahashi, and H. Suda, "Wideband DS-CDMA for next generation mobile communication systems," *IEEE Communications Magazine*, pp. 56–69, September 1998.

[6] M. McTiffin, A. P. Hulbert, T. J. Ketseoglou, W. Heimsch, and G. Crisp, "Mobile access to an ATM network using a CDMA air interface," *IEEE J. Sel. Comm.*, vol. 12, pp. 900–908, June 1994.

[7] M. Saquib, R. Yates, and N. Mandayam, "Decorrelating detectors for a dual rate synchronous DS/CDMA channel," *Wireless Personal Comm.*, vol. 9, no. 3, pp. 197–216, 1998.

[8] J. Chen and U. Mitra, "Analysis of decorrelator-based receivers for multi-rate CDMA communications," *IEEE Trans. Veh. Tech.*, vol. 48, pp. 1966–1983, November 1999.

[9] M. Juntti, "Multiuser detector performance comparisons in multirate CDMA systems," in *Proceedings of the 1998 48th IEEE Vehicular Technology Conference*, vol. 1, (Ottawa, Can), pp. 31–35, May 1998.

[10] S. Buzzi, M. Lops, and A. M. Tulino, "MMSE multiuser detection for asynchronous dual-rate direct sequence CDMA communications," in *the Ninth IEEE Int. Symp. Personal, Indoor and Mob. Radio Comm.*, vol. 1, pp. 223–227, 1998.

[11] U. Mitra, "Comparison of maximum-likelihood based detection for two multi-rate access schemes for CDMA signals," *IEEE Transactions on Communications*, vol. 47, pp. 64–77, January 1999.

[12] A.-L. Johansson and A. Svensson, "On multirate DS/CDMA schemes with interference cancellation,," *J. Wireless Personal Comm.*, vol. 9, pp. 1–29, January 1999.

[13] T. Ojanpera and R. Prasad, "An overview of air interface multiple access for IMT-2000/UMTS," *IEEE Communications Magazine*, pp. 82–95, September 1998.

[14] A. Sabharwal, U. Mitra, and R. Moses, "Cyclic Wiener filtering based multirate DS-CDMA receivers," in *Proc. of IEEE WCNC*, (New Orleans, LA), Sept. 1999.

[15] W. A. Gardner, "The structure of least-mean-square linear estiimators for synchronous M-ary signals," *IEEE Trans. Info. Th.*, pp. 240–243, March 1973.

[16] E. Biglieri, M. Elia, and L. Lopresti, "The optimal linear receiving filter for digital transmission over nonlinear channels," *IEEE Trans. Info. Th.*, vol. 35, May 1989.

[17] A. Sabharwal, U. Mitra, and R. Moses, "MMSE receivers for multirate DS-CDMA systems," *submitted to IEEE Trans. Comm.*, Jan. 2000.

[18] D. G. Luenberger, *Optimization by Vector Space Methods.* New York: Wiley, 1969.

[19] W. A. Gardner, "Cyclic Wiener filtering : theory and method," *IEEE Trans. Comm.*, vol. 41, pp. 151–163, Jan. 1993.

[20] R. A. Horn and C. R. Johnson, *Matrix Analysis.* Cambridge, 1985.

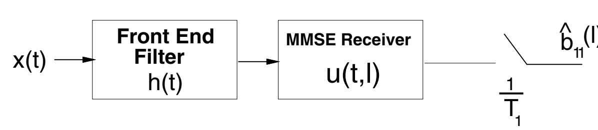

Fig. 1: Receiver structure.

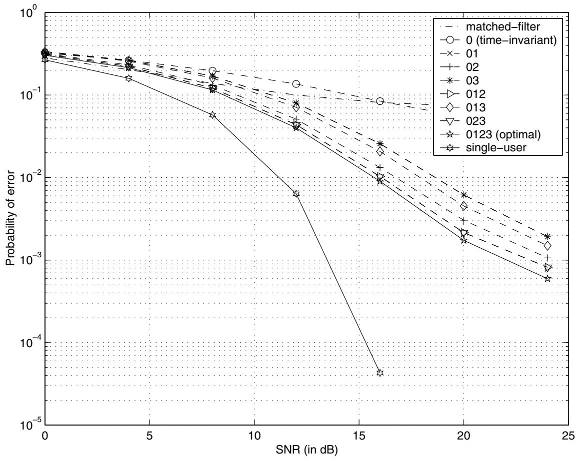

Fig. 2: Probability of error versus SNR for user 11 using the matched filter, seven suboptimal receivers with different set of cycle frequencies and the optimal receiver; single user bound is also given for comparison.

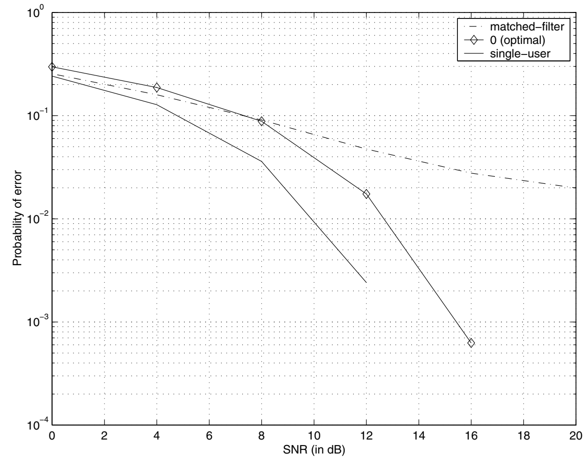

Fig. 4: Probability of error versus SNR for user 13 using the matched filter and the optimal receiver which is time-invariant in this case; single user bound is also given for comparison.

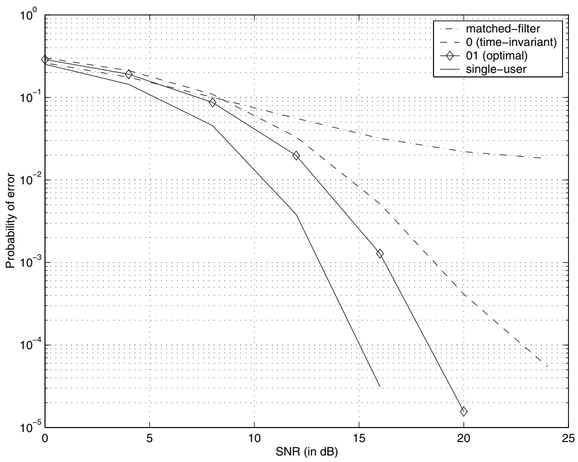

Fig. 3: Probability of error versus SNR for user 12 using the matched filter, suboptimal time-invariant receiver and the optimal receiver; single user bound is also given for comparison.